Chapter 16

Feasibility and Numerical Analysis of Hybrid Photovoltaic (PV) Panels with Thermoelectric Cooling (TEC) Systems

Arturo Monedero Khouri and
Miguel Angel Olivares Robles

Additional information is available at the end of the chapter

http://dx.doi.org/10.5772/intechopen.75441

Abstract

Photovoltaic-thermoelectric hybrid (PV-TE) systems combine photovoltaic (PV) cells and thermoelectric cooling (TEC) modules to improve the system performance. PV panels efficiency is undesirably influenced by temperature rise, reducing power outlet from PV cells. As a countermeasure, cooling methods have been widely suggested. In this chapter, we provide an overview of both technologies, as well as an analysis of thermoelectric cooling as a possible solution to temperature rise in PV panels. Energy and exergy balances of hybrid system are conducted to determine if the thermoelectric cooling is viable for a self-sustaining system. Our results show that copper indium gallium selenide (CIGS), crystalline silicon (c-Si), amorphous silicon (a-Si), and cadmium tellurium (CdTe) PV panels are unsuitable candidates using the TE cooling. Even though exergy losses diminish with temperature decrease in CIGS, c-Si, and a-Si, the power consumption of the TEC has shown to overcome power generation from PV panels.

Keywords: thermoelectrics, cooling, photovoltaics, hybrid, exergy

1. Introduction

When talking about photovoltaics we are referring to a technology that generates a direct current from semi-conducting materials arranged in cells when they are illuminated by photon particles [1]. These cells generate electrical power for as long as light is shined upon them.

PV effect was first observed by Heinrich Hertz in the late 1800s and has come across power generating devices by early 1900s [2]. It only became more relevant with *positive-negative* (*pn*) junction discovery, consolidating the development of solar photovoltaic panels [1]. Ever since, efficiency has been a paramount factor to be optimized and, as technology advanced and efficiency increased, the diffusion of PV panels has reached worldwide popularity.

1.1. Basic concepts of PV cells

Incident light can be conceived as a stream of photons at a determined frequency. A photon, is a particle of electromagnetic energy, this energy contained by the photon follows the equation:

$$E_{photon} = h\nu \tag{1}$$

where E_{photon} is the energy of the photon, h is Planck's constant ($6.626{*}10^{-34}\ Js$), and ν is the light frequency [3]. When photons with an appropriate frequency, incoming from the shined light, hit a metal surface, electrons in the metal absorb the photons' energy and are knocked off. This energy of the photon transferred to the electron is conserved. An amount is used to knock off the electron (Φ), this term is known as *work function* and varies according to the metal employed, and the remaining energy is transformed into kinetic energy for the electron ($K_{electron}$).

$$E_{photon} = K_{electron} + \Phi \tag{2}$$

This *work function* Φ is the minimum energy required to knock off an electron from a metallic surface, and its value is given by the metallic material. As photons' energy is determined by their frequency, the minimum frequency required to match the *work function* is known as the threshold frequency (ν_0), and for frequencies greater than ν_0, electrons hit will be ejected [3], producing a current flow.

As depicted in **Figure 1**, the frequency of red light (left) is a lesser value than the threshold frequency (ν_0) required to knock off electrons, so none are ejected. The green and blue frequencies of moderate and short wavelengths respectively have ($\nu > \nu_0$) causing photoemission. Higher frequencies correspond to higher kinetic energy acquired by the electrons as they are ejected.

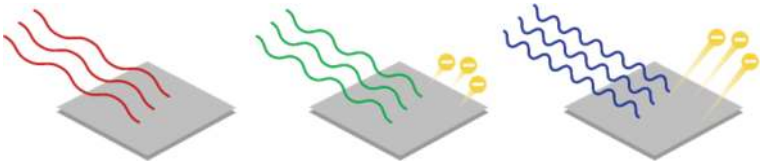

Figure 1. Different frequencies/wavelengths result in none, slower or faster electron ejection from the metal surface as protons collide with it [4].

1.2. PV efficiency as a function of temperature

As discussed before, materials are determinant for the energy amount required to knock off electrons and start a current flow. Different material compounds will possess distinctive photoelectric properties. We can think of this diversity as the stress resistance an alloy possesses; different alloys will have diverse behaviors when submitted to stress conditions, just as different material combinations will allow various photoelectric characteristics.

The paramount property when looking for photoelectric materials is efficiency (η). With higher efficiencies, more incident sunlight will be effectively converted into exploitable electrical power. This relationship between the net electrical power delivered by the PV panel (P_{PV}) and its efficiency (η_{PV}) can be expressed as:

$$P_{PV} = \eta_{PV} Q_{solar} \tag{3}$$

where Q_{solar} is the total incident sunlight shined upon the panel's surface.

Nonetheless, PV panel efficiency is influenced not only by the material's properties, but it can also vary due to temperature changes regardless of the material composition. The drop in efficiency as temperature rises can be traced to the influence upon current and the voltage; as it turns out, the thermally excited electrons begin to dominate the electrical properties of the semi-conductor [5] describing a linear relation for the PV efficiency in the form:

$$\eta_{PV} = \eta_{T_{ref}} \left(1 - \gamma \left(T_{cell} - T_{ref}\right)\right) \tag{4}$$

in which $\eta_{T_{ref}}$ is the cell efficiency at the reference temperature T_{ref}, typically 25°C, and γ represents the temperature coefficient, which can be found in **Table 1** for the several types of PV modules analyzed. These values are usually given by the manufacturer, but can also be calculated with:

$$\gamma = \frac{1}{T_0 - T_{ref}} \tag{5}$$

for which T_0 is the temperature at which the PV panel's efficiency drops to zero.

1.3. Why choose PV panels?

Back in 1997, the largest panels available were 100 W panels, each was around 9% efficient; the cost oscillated around $1300 apiece. Today, solar panels can be up to 24% efficient and cost 25 times less. They also have a higher capacity and a longer life expectancy. Of course, there is more to the installation cost than just the solar panels alone. Cabling, inverters, batteries, mounting brackets and time all cost money, and most of those prices have increased in the past 20 years, but the fact remains that solar has been transformed from an obscure niche product to mainstream energy generation because of incredible leaps in the technology that has made solar more efficient and affordable [6].

Parameters	Symbol	Value
Ambient temperature	T_{amb}	293 K
Area of PV panel	A_{cell}	0.4 m^2
Area of thermoelectric module	A_{TE}	0.04 m^2
Characteristic longitude	L_C	0.6325 m
Efficiency of PV panel at reference temperature	$\eta_{T_{ref}}$	
CdTe		27.9%
CIGS		13.3%
c-Si		12.4%
a-Si		5.0%
Emissivity of the ground	ϵ_{ground}	0.2
Emissivity of the sky	ϵ_{sky}	0.9
Gravity's acceleration	g	9.81 m/s^2
Reference temperature	T_{ref}	298 K
Reflected radiation fraction	ρ_{opt}	0.12
Stephen-Boltzmann constant	σ	$5.6704{*}10^{-8}$ W/m^2K^4
Solar incidence	G	700 W/m^2
Sun temperature	T_{sun}	6000 K
Temperature coefficient	γ	
CdTe		0.00205 K^{-1}
CIGS		0.00353 K^{-1}
c-Si		0.00392 K^{-1}
a-Si		0.00110 K^{-1}
Thermal conductivity (air)	k	0.02587 W/mK
Thermal diffusivity (air)	α	0.00002163 m^2/s
Thermal expansion coefficient (air)	β	0.00324 K^{-1}
Tilt angle	θ	45°
Wind speed	w	2 m/s

Table 1. Parameters of the PV-TEC hybrid system.

Nonetheless, several studies throughout the years have established that temperature increase in PV cells result in efficiency decrease [7–10]. Hence, power output of a PV panel decreases with temperature increment. This is the reason for cooling devices as key component of an integrated hybrid generation system. As PV panels are only capable to convert sunlight or luminous energy into electrical energy, any heat contained in the system will result in an ill temperature rise with counterproductive results. For this purpose, thermoelectric technology

http://dx.doi.org/10.5772/intechopen.75441

has come to our attention, offering a compact solution for the cooling problem that has been previously discussed.

1.4. Thermoelectrics

An electrical potential, also known as voltage, is generated within two dissimilar conducting materials subjected to a temperature gradient. The conversion of this electric voltage differences into temperature gradients and vice versa is known as the thermoelectric effect [11]. It is composed by three different phenomena: the Seebeck effect, the Peltier effect, and the Thomson effect. These can be used to generate electricity, measure temperature, and as a heat source/pump.

1.4.1. The Seebeck effect

An electrical current is originated when an electrical circuit consisting of two dissimilar metals has a temperature difference between its joints. This kind of arrangement is known as *thermocouple* and is usually composed of p-doped and n-doped semiconductors, as depicted in **Figure 2a**.

The Seebeck effect is a typical example of an electromotive force (emf), modifying Ohm's law:

$$V = \propto \Delta T \tag{6}$$

where $\propto$ is the Seebeck coefficient, a property inherent to the local material, also known as themorpower, and ΔT is the temperature gradient between the heat source and the cool side.

1.4.2. The Peltier effect

Complementary to the Seebeck Effect, when a current is passed through an electrical circuit consisting of two dissimilar metals, heat may be generated or removed at the junction as shown in **Figure 2b**. Heat generation or removal will alternate in the junctions if the direction of the current flow is reversed.

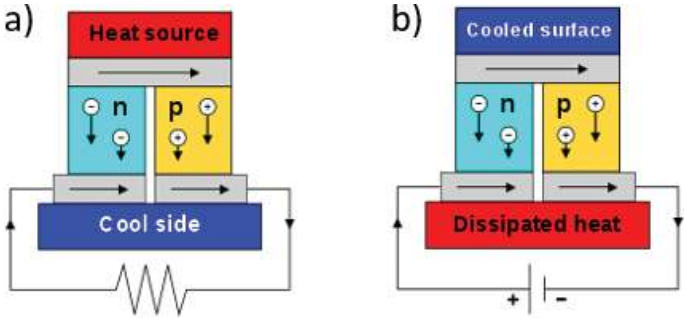

Figure 2. A thermoelectric circuit composed of dissimilar materials, configured as a thermoelectric generator (a) [12] and as a thermoelectric cooler (b) [13].

The Peltier heat generated at the joints per time unit is:

$$\dot{Q} = (\Pi_A - \Pi_B)I \tag{7}$$

where $\dot{Q}$ is the heat flow, Π_A and Π_B are the Peltier coefficients of conductors, and I is the electric current (from A to B).

1.5. TECs performance as a function of temperature

Thermoelectric modules can operate as electrical energy generators or heat pumps, commonly known as cooling devices. The efficiency for these modules benefits from high temperature gradients (ΔT) while generating electrical energy, somewhat around 300°C for most devices. On the other hand, cooling thermoelectric coefficient of performance (COP) is increased when small temperature gradients are present between the body that's been cooled and the ambient temperature.

While on cooling mode, TEC modules consume energy, removing heat from a particular source and releasing it into the medium. This heat removal and energy consumption differ greatly in behavior depending on the thermocouple materials. For the analysis presented here, a commercial module HP-199-1.4-1.15 from TE Technology, Inc. has been implemented. The technical specifications and fitting data were taken from its datasheet presented in **Figure 3**. Equations (8) and (9) have been fitted to this data, considering a hot side temperature of 50°C and 10.2 V circuit voltage.

$$Q_{removed} = -1.4557\Delta T + 67.004 \tag{8}$$

$$I_{TEC} = -0.0185\Delta T + 3.213 \tag{9}$$

Additional to this heat removal, TEC module consumes energy, which is not necessarily the same amount as heat removes. This power consumption is the product of the circuit voltage (V_{TEC}) and the input current (I_{TEC}).

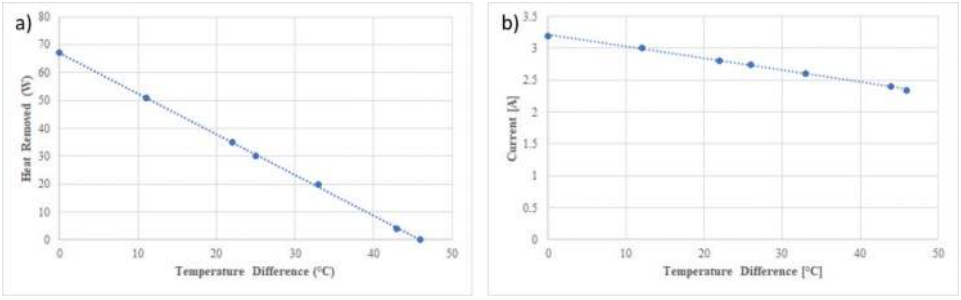

Figure 3. Amount of heat removed (a) and magnitude of current demanded (b) by a commercial HP-199-1.4-1.15 thermoelectric cooler as a function of the temperature gradient between the heat source (T_{cell}) and the heat sink (T_{amb}) as specified by its data sheet.

$$P_{module} = V_{TEC} I_{TEC} \tag{10}$$

Equations (9) and (10) account only for a single TEC module. For calculating the number of TEC modules required, the heat to be removed must be found (Q_{cool}) from Eq. (14). Then the quotient from $Q_{removed}$ and Q_{cool} can be used to determine the number of TEC modules (n_{TEC}) required for the cooling, and then multiplied by each individual consumption to find the total power consumed by the array.

$$n_{TEC} = \frac{Q_{cool}}{Q_{removed}} \tag{11}$$

$$P_{TEC} = P_{module} n_{TEC} \tag{12}$$

where P_{module} is the power consumed by each TEC module, and P_{TEC} is the total power consumed by all TEC modules for cooling.

1.6. Why choose thermoelectrics?

It is established by the Peltier effect that heat is absorbed or liberated when current crosses an interface, given the direction of the current flow, between two different conductors [11], laying the foundations for TEC modules. These constitute miniature devices, unlike conventional vapor systems, energized by a DC power input. Additional to the weight and space savings carried by TECs, their solid-state construction is fluid free to operate and highly reliable, offering also a precise temperature control [14].

In this chapter, we will structure a theoretical frame for the energy inputs and outputs of a PV+TEC hybrid as a brief overview. Then, we will turn out attention to the operational feasibility of the hybrid system, using an energy and exergy balance as assessment. Finally, results of our simulations as well as conclusions will be presented and discussed in depth.

2. Theoretical frame

First, we consider the studied system to be analyzed: a solar PV panel shined upon by sunlight, while cooled through a commercial thermoelectric module (HP-199-1.4-1.15) with previously defined working conditions, see **Figure 4**. Normal convection and radiation take place, as well as sunlight rejection from the PV panel's surface. Also, the system has reached a steady-state condition, meaning that the previously mentioned variables defining the system are unchanging in time.

During steady-state conditions, the total amount of energy remains constant; thus, the total energy change in the system equals zero ($\Delta E_{sys} = 0$) [15]. In consequence, the amount of energy entering the system must be equal to the amount of energy leaving the system. And so, the general energy balance is reduced to:

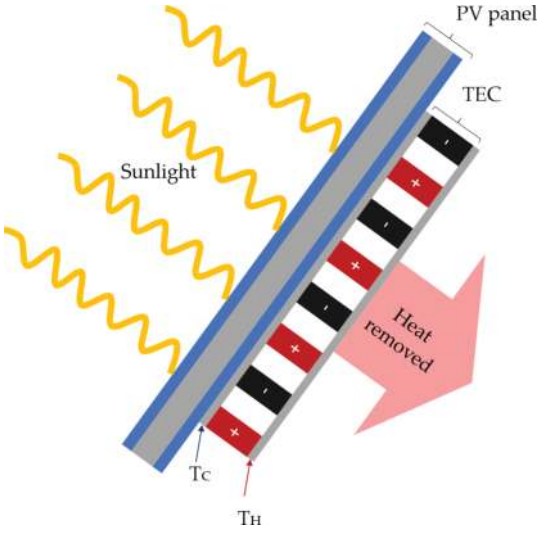

Figure 4. Schematic of the PV+TEC assembly.

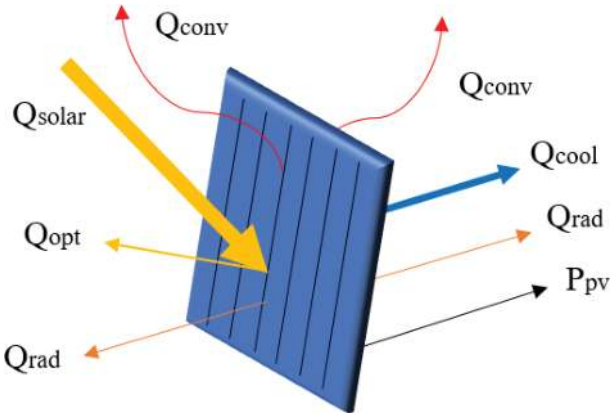

Figure 5. Schematic of the PV+TEC energy inputs and outputs.

$$\dot{E}_{in} - \dot{E}_{out} = 0 \tag{13}$$

Different energy inputs and outputs are outlined entering and leaving the hybrid PV-TEC system, as can be appreciated in **Figure 5**. The sunlight irradiates the panel (Q_{solar}) continuously, this luminous energy is either absorbed or reflected (Q_{opt}) by the PV panel surface. The absorbed fraction is then transformed into electrical energy (P_{PV}) and heat. Some of this heat will be dissipated passively, this means that no energy inputs will be required to extract it from

the system, on each side of the cell by natural cooling mechanisms such as convection (Q_{conv}) and radiation (Q_{rad}).

If we left the system to cool passively, a temperature around 60–80°C is expected to be reached [16]. But in this scenario, a cooling system is implemented to reduce its temperature even more. The thermoelectrical cooler will extract another energy fraction (Q_{cool}) from its contact surface with the PV panel at T_C, while consuming electrical power, and release it to its surroundings passively through its rear end at T_H, no additional components passive or active are considered heat extraction, for example heat exchangers. Thus, considering Eq. (13), the energy balance equation for the hybrid system in steady-state conditions can be written as follows:

$$Q_{solar} = Q_{opt} + Q_{conv} + Q_{rad} + P_{PV} + Q_{cool} \tag{14}$$

Each term is determined by several factors, such as panel characteristics, ambient temperature, wind speed, solar radiation conditions, etc. [17]. These system parameters are shown in **Table 1** and will be employed in further equations. Each term in Eq. (14) is determined by a theoretical model which will be described in the sections to come.

2.1. Solar radiation model

Solar irradiance varies significantly from one place to another and changes throughout the year [6]. The values considered for this model in **Table 1** were selected considering a standard setting for solar irradiance and tilt angle. This selected data is input into the following equation to calculate Q_{solar} and Q_{opt}.

$$Q_{solar} = GA_{cell} \tag{15}$$

It is to be noted that part of Q_{solar} is reflected by the solar panel materials, thus never entering the system. This fraction of reflected radiation is commonly expressed as ρ_{opt} and used to calculate the optical losses (Q_{opt}) of sunlight radiation.

$$Q_{opt} = Q_{solar}\rho_{opt} \tag{16}$$

As stated before, the net solar energy ($Q_{solar} - Q_{opt}$) entering the system will be transformed into electrical power (P_{PV}) and heat. This heat is dissipated by several mechanisms such as convection, radiation, and the thermoelectrical cooling module.

2.2. Convective heat model

As heat accumulates in the system, temperature rises, creating a temperature differential between the system and its surroundings. This originates a heat exchange between the system and the surrounding air known as convective heat loss. There are two phenomena accountable for heat loss: forced and natural convection; these must be considered for the front and the rear faces as the air surrounds the plate from both sides.

Natural convection is related to the temperature difference between the outside air and the panel, which includes the movement of the fluid due to the local density gradients. In calm or little windy days, the contribution of natural convection becomes significant, even more in cold climates where temperature differences between the panel surface and ambient air can be relatively large [17]. Forced convection, in the other hand, relates to the presence of the wind. There are numerous studies on the evaluation of the heat transfer coefficients due to this phenomenon, some are studies in wind galleries, others on field measurements, nonetheless several authors found that the theory usually underestimates the presence of different objects near the panels (other panels, trees, soil, buildings, etc.) [17].

The small area in between the two faces is rendered negligible, and the plate is considered as an isothermal surface for simplification purposes [18]. This allows us to define the convective heat loss as:

$$Q_{conv} = Q_{conv,front} + Q_{conv,rear} \tag{17}$$

$$Q_{conv,front} = h_{conv,front} A_{cell} (T_{cell} - T_{amb}) \tag{18}$$

$$Q_{conv,rear} = h_{conv,rear} A_{cell} (T_{cell} - T_{amb}) \tag{19}$$

where h_{conv} is the overall convective heat coefficient, A_{cell} is the PV panel surface, and $(T_{cell} - T_{amb})$ is the temperature gradient between the cell surface and the ambient temperature. A_{cell}, T_{cell}, and T_{amb} are constant values that can be found in **Table 1** as system parameters. Nonetheless h_{conv} must be calculated, considering natural and forced convection into the same coefficient for each panel side:

$$h_{conv,front} = \sqrt[3]{h_{natural,front}{}^3 + h_{forced,front}{}^3} \tag{20}$$

$$h_{conv,rear} = \sqrt[3]{h_{natural,rear}{}^3 + h_{forced,front}{}^3} \tag{21}$$

To determine forced convection heat transfer coefficient, wind speed (w) is a key variable, this parameter can also be found in **Table 1**. A model developed by Sharples and Charlesworth methodology [19] is applied to the system.

$$h_{forced,front} = 3.3w + 6.5 \tag{22}$$

$$h_{forced,rear} = 2.2w + 8.3 \tag{23}$$

This leaves natural convection heat transfer coefficient remaining. For it, the Nusselt (Nu) number concept must be analyzed first. The Nusselt number, named after Wilhelm Nusselt, establishes the ratio of convective to conductive heat transfer [20] and, as it may be inferred, it's dimensionless.

$$\overline{Nu} = \frac{Q_{conv}}{Q_{cond}} = \frac{L_c h_{natural}}{k} \tag{24}$$

where $h_{natural}$ is the natural convective coefficient for the fluid, k the fluid's thermal conductivity, and L_c the characteristic longitude of the surface. Nusselt numbers are usually determined empirically for different configurations such as horizontal or inclined flat surfaces, spherical and cylindrical objects, enclosures, etc. The PV panel configuration resembles that of an inclined plane, for which Fujii and Imura model [21] as well as Churchills and Chu's [21] are suggested to be implemented.

$$\overline{Nu}_{front} = 0.14\left[(Ra)^{\frac{1}{3}} - (Ra_{cr})^{\frac{1}{3}}\right] + 0.56(Ra_{cr}\cos\theta)^{\frac{1}{4}} \tag{25}$$

$$\overline{Nu}_{rear} = \left[0.825 + \frac{0.387Ra^{\frac{1}{6}}}{\left[1 + \left(\frac{0.492}{\Pr}\right)^{\frac{9}{6}}\right]^{\frac{8}{27}}}\right]^2 \tag{26}$$

where θ is the tilt angle between the ground and the rear surface of the panel, Ra is the Raleigh number for the fluid's conditions, and Ra_{cr} is the critical Raleigh number at which the Nusselt starts deviating from the laminar relationship ($Ra_{cr} \approx 10^9$).

$$Ra = \frac{g*\beta(T_{cell} - T_{amb}){L_c}^3}{\nu\alpha} \tag{27}$$

where g is gravity's acceleration, β is the fluid's thermal expansion coefficient, ν is the fluid's kinematic viscosity, and α is the fluid's thermal diffusivity. These values are given as system parameters in **Table 1** for air as work fluid.

2.3. Radiation heat model

Thermal radiation is associated with the rate at which matter emits energy as a result of its finite temperature [20]. The assessment of the radiation heat model contemplates radiation emitted to the sky and radiation emitted to the ground from the front and rear faces of the PV panel. This, as seen before in the convective model, divides the heat flow into several components.

$$Q_{rad} = Q_{rad.sky,\,front} + Q_{rad.sky,\,rear} + Q_{rad.ground,\,front} + Q_{rad.ground,\,rear} \tag{28}$$

This radiation emissions are originated by the energy released due to oscillations of the many electrons constituting the matter [20]. Different bodies will emit different amounts of radiation, even at the same temperature, introducing the concept of emissivity (ϵ), which is the ratio between the emitted radiation by a body's surface at a given temperature and the radiation emitted by a *black body* at the same temperature [22]. This *black body* is defined as the perfect emitter and absorber body, emitting a radiation per area unit of:

$$E_b(T) = \sigma T^4 \tag{29}$$

where $\sigma = 5.670*10^{-8}\ W/m^2K^4$, known as the Stephen-Boltzmann constant. Using equation along with emissivity values found in **Table 1**, and a geometrical factor F considering an incline plate, the radiative model components can be written:

$$Q_{rad,\,sky,\,front} = F_{sky,\,front}\epsilon_{sky}\sigma A_{cell}\left({T_{cell}}^4 - {T_{amb}}^4\right) \tag{30}$$

$$Q_{rad,\,sky,\,rear} = F_{sky,\,rear}\epsilon_{sky}\sigma A_{cell}\left({T_{cell}}^4 - {T_{amb}}^4\right) \tag{31}$$

$$Q_{rad,\,ground,\,front} = F_{ground,\,front}\epsilon_{sky}\sigma A_{cell}\left({T_{cell}}^4 - {T_{amb}}^4\right) \tag{32}$$

$$Q_{rad,\,ground,\,rear} = F_{ground,\,rear}\epsilon_{sky}\sigma A_{cell}\left({T_{cell}}^4 - {T_{amb}}^4\right) \tag{33}$$

for which the geometrical factor F is given as:

$$F_{sky,\,front} = \frac{1}{2}(1 + \cos\theta) \tag{34}$$

$$F_{sky,\,rear} = \frac{1}{2}(1 + \cos(\pi - \theta)) \tag{35}$$

$$F_{ground,\,front} = \frac{1}{2}(1 - \cos\theta) \tag{36}$$

$$F_{ground,\,rear} = \frac{1}{2}(1 - \cos(\pi - \theta)) \tag{37}$$

3. The hybrid system

This work's goal is to elaborate a net energy balance between PV generated energy and TEC consumed energy. In fact, we show that TEC's consumed power is greater than PV generated power in all temperature ranges, except for the CdTe PV panel at some temperature ranges. Other works focus in the PV efficiency increase only, disregarding TEC energy consumption associated to it, which makes difficult to assess the energy balance of the hybrid system.

Some of this works can be traced to authors like Najafi and Woodbury [23] who use a modeling approach. Likewise, Borkar, Prayagi and Gotmare [24] report, from a MATLAB simulation model, that increase in life span and efficiency can be achieved by PV + TEC systems without mentioning the net hybrid system energy balance.

Another example of this is the work of Kane and Verma [25] model, with reported results of 0.45% increase in efficiency per °C. This behavior is already expected from a solar PV panel, as explained by Eq. (4), where any temperature decrease will result in a power increase from the module; raising the question: *does the increment in power generation results convenient in comparison with power consumed by TEC cooling to reduce temperature in the PV module?*

Additionally, an experimental montage was elaborated by Benghanem, Al-Masharaqi and Daffallah [26] with a 0.5% of efficiency increase per °C decreased, conducted at Madinah, Saudi Arabia, where panel temperatures rise to 83°C. Results show great resemblance to those of Kane and Verma, but continue to leave aside the analysis for the energy consumption of the active cooler.

Analogue considerations to the work developed by Bjørk and K. Nielsen [27] Analysis for PV and thermoelectric generator (TEG) systems were employed throughout this chapter, where the efficiency of such a hybrid system cannot be considered as single stand-alone units and thus its power generation characteristics are not known. In addition to this approach, it is to be noted that TEGs were replaced with TECs, and real approximation conditions were considered along with an exergy analysis.

A combined PV+TEC system is analyzed regarding a real approximation. The goal for this kind of system is to be a source of electrical power, meaning that power generated by the PV panel must overcome energy consumption from the TEC at all times to ensure its operational validity, otherwise the system will be consuming a greater amount of power than it is able to generate.

$$P_{gen} > P_{cons} \tag{38}$$

$$W_{net} = P_{gen} - P_{cons} > 0 \tag{39}$$

For the proposed system and its limits, as depicted in **Figure 6**, the means for power generation are the PV cells, and the power consuming means are the TECs. The system proposal

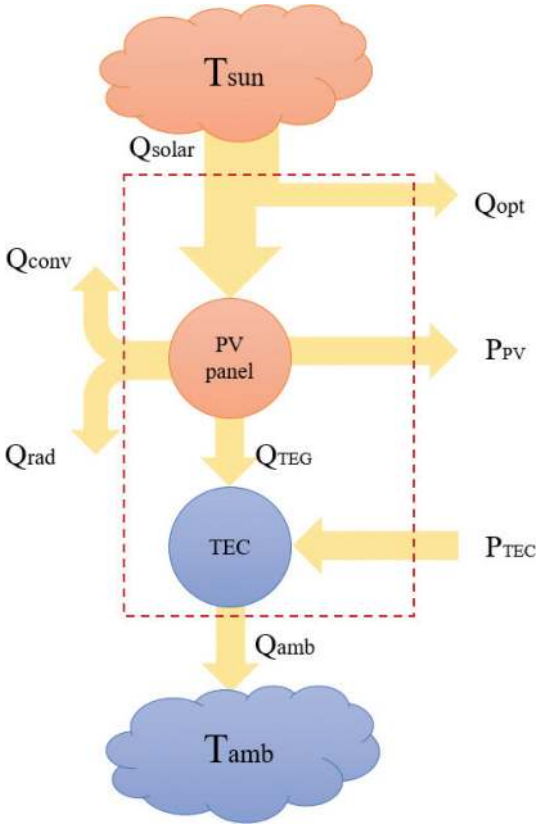

Figure 6. Schematic of the PV+TEC hybrid system limits and energy balance.

intends to assess for the PV panels change in efficiency as temperature is lowered following the working principles of Eqs. (3) and (4) and with the energy consumption of the increasing number of TECs, determined by Eqs. (11) and (12). As active and passive cooling mechanisms extract heat from the hybrid system, energy losses are intended to be found, watching W_{net}'s behavior to determine if the hybrid system is generating enough energy to compensate and justify its active cooling means and account for its feasibility as a power generating system. A net metering method of produced and consumed energy will allow us to determine if $P_{PV} > P_{TEC}$, which must be fulfilled to ensure a $W_{net} > 0$.

3.1. Hybrid system exergy balance

Additional to the energy balance simulations, exergy analysis is undertaken. Considering the same operational temperature range as the energy balance simulations, the temperature of least entropy is intended to be found by the model.

As we know, every engineering processes performance is degraded by system irreversibilities associated to non-ideal conditions. Entropy is a quantitative measure of this irreversibilities; with greater irreversibilities comes greater entropy generation, which means valuable energy is lost in the process [15]. Of course, not all lost energy can be recovered, as the system conditions are not those of a theoretical reversible machine, nonetheless exergy analysis provides a tool for analyzing the minimum entropy generation that can be achieved by a real model, and thus the maximum energy output that can be obtained.

Exergy balance for the PV + TEC hybrid system contemplates all the exergy entering (X_{in}) and exiting (X_{out}) the system, and the destroyed exergy (X_{loss}), by irreversibilities, during the process:

$$X_{in} = X_{out} + X_{loss} \tag{40}$$

The only input to the system, as shown in **Figure 6** and Eq. (14) is solar radiation, expressed as:

$$X_{in} = GA_{cell}\psi_s \tag{41}$$

where ψ_s is the exergy efficiency of solar radiation [28]. This exergy efficiency is the maximum efficiency ratio of the solar emission, and can be calculated with:

$$\psi_s = 1 + \frac{1}{3}\left(\frac{T_0}{T}\right)^4 - \frac{4}{3}\left(\frac{T_0}{T}\right) \tag{42}$$

for this case of study, temperature of the radiation source T, is the Sun's surface temperature (T_s), and T_0 is the baseline temperature at which the system is referred (T_{amb}) [29].

Heat is an unorganized form of energy, and there's just a limited amount that can be transformed into organized energy such as work. It is always possible to produce work from a temperature source whose temperature is higher than the surroundings, in response, this

heat transfer, will always come with exergy transfer [15]. A heat flow Q coming from a thermal source of temperature T will always be accompanied by an exergy transfer X_{heat} of the amount:

$$X_{heat} = \left(1 - \frac{T_0}{T}\right)Q \tag{43}$$

Exergy is a unit for measuring the potential useful work, meaning that any exergy transfer done by work will be equal to the amount of work itself.

$$X_{work} = W \tag{44}$$

Irreversibilities such as friction, mixing, chemical reactions, heat transfer, expansion, compression, etc., will always generate entropy, and everything that generates entropy destroys exergy [15]. Exergy losses represent the wasted work potential, caused by the irreversibility of the process of energy conversion. Any real process will have destroyed exergy, while only ideal scenarios will present $X_{loss} = 0$. The hybrid system involves several exergy losses such as:

$$X_{loss} = X_{loss,\,opt} + X_{loss,\,sur} + X_{loss,\,solar} + X_{loss,\,TEC} \tag{45}$$

Each process in which energy is transferred and transformed presents irreversibilities, thus every term enlisted in Eq. (45) has exergy loss due to these inefficiencies in energy conversion. The first term ($X_{loss,\,opt}$) we called optical loss caused by the absorption and reflection of sunlight. The second term ($X_{loss,\,sur}$) is caused by the heat exchange between the system and its surroundings by the convective phenomenon, both natural and forced. The third term ($X_{loss,\,solar}$) is generated when the high-grade solar radiation is converted into low-grade thermal energy. Finally, the last term is caused by the TEC module consuming electric power, which is defined as exergy itself, and expelling heat from the hybrid system.

$$X_{loss,\,opt} = GA_{cell}\psi_s\rho_{opt} = X_{in}\rho_{opt} \tag{46}$$

The surface of the hybrid system is always at a higher temperature than its surroundings, thus the heat exchange remains continual if sunlight keeps irradiating the PV panel surface. According to the definition of exergy transfer as heat flow, and using the ambient temperature as reference the following can be obtained

$$X_{loss,\,sur} = (Q_{rad} + Q_{conv})\left(1 - \frac{T_{amb}}{T_{cell}}\right) \tag{47}$$

note that the higher the difference between T_{cell} and T_{amb}, the more exergy is lost.

The process of transforming solar radiation into electrical power and thermal energy is an irreversible process, and its exergy loss can be calculated with

$$X_{loss,\,solar} = GA_{cell}\psi_s - X_{loss,\,opt} - X_{loss,\,sur} - P_{PV} - Q_{cool}\left(1 - \frac{T_{amb}}{T_{cell}}\right) \tag{48}$$

Finally, exergy is defined as useful work, and the TEC consumes electrical power to operate, as well as it expels a given heat flow. Thus, an exergy loss is being held at it. To consider this into the balance, the following relation was used

$$X_{loss,\,TEC} = Q_{cool}\left(1 - \frac{T_{amb}}{T_{cell}}\right) + P_{TEC} \tag{49}$$

4. Simulations

We now focus our attention on P_{PV} in Eq. (3), P_{TEC} in Eq. (12), and the energy balance as well as Q_{cool} in Eq. (14). The Q_{cool} heat flux determined by the energy balance of the system will define the amount of TEC modules required to cool the system, enhancing the P_{PV} efficiency as established in Eqs. (3) and (4).

A temperature interval from 333 to 298 K was used for the system evaluation. This interval was chosen regarding the average temperature of a PV panel without cooling (333 K) [16] and a typical value for reference temperature used for PV panel evaluation (298 K).

Based on an energy analysis, the system's feasibility was assessed. We compared the PV panel power generation and the TEC energy consumption for each type of PV module. The power is shown in **Figure 7a** for a TEC+CIGS PV coupling, **Figure 7b** for TEC+c-Si, **Figure 7c** for TEC+a-Si array, and **Figure 7d** for TEC+CdTe. A general PV power generation increase of 10.22% is observed. If we put this quantity in perspective with each °C decreased we'll obtain

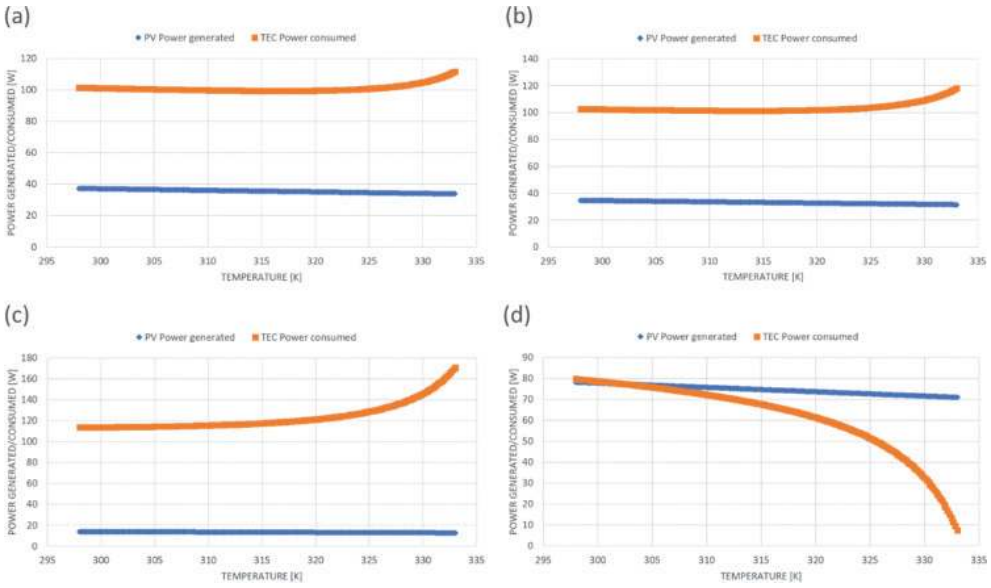

Figure 7. The energy generation for a PV panel compared to the consumption of the TEC in the same system montage. (a) TEC+CIGS power generation vs. consumption, (b) TEC+C-SI power generation vs. consumption, (c) TEC+A-SI power generation vs. consumption, (d) TEC+CDTE power generation vs. consumption.

a 0.292% climb in PV efficiency per °C, comparable to the results found by Kane and Verma [25] and Banghanem, Al-Mashraqi and Daffalah [26].

As can be seen from the figures, except in the case of CdTe, the cooling modules demand a much higher amount of power than what has been produced by the system at all temperatures; even when the efficiency of the PV panel does climb and the TEC consumption decreases, the ratios are not as elevated as it would be necessary for W_{net} to be positive at any point, as intended, according to Eq. (39). The diminishment in TECs power consumption can be traced to net power consumed and number of modules employed, where: CIGS decreased 9.14% the power consumption from the highest to the lowest temperature and reduced 1.238 TECs (n_{TEC}) use needed to cool the system, using Eqs. (8) through (12). These results were consistent with c-Si with 12.97% reduction in power consumption and 1.45 fewer TEC modules, as well as a-Si with 33.43% less power consumption and 3.195 unneeded modules.

Regarding the abnormal behavior of TEC+CdTe system, the curves shown in **Figure 7d** explain that the TEC consumption plummets at high ΔT values. If we concentrate our attention in each term of the system's energy balance (Eq. (14)) we can notice that Q_{solar} and Q_{opt} are not temperature dependent, whereas Q_{conv} and Q_{rad} will contribute in heat dissipation in the same amount for any type of PV+TEC system, leaving P_{PV} and Q_{cool} to account for this odd behavior. After a careful analysis we can only conclude that a small amount of heat removal is required at initial ΔT values. Contrary to the other systems, TEC energy consumption increases when the system approaches (T_{amb}), resulting astoundly counterproductive.

Contrary to the rest of the systems, CdTe doesn't decrease the TECs consumption as it cools, on the opposite, results report almost 9.5 times more energy consumption due to the cooling, and 7.5 more modules required than it did at initial temperatures (333 K). When approximating ambient temperature (298 K) in **Figure 7b**, almost all power generated by the PV panel can be appreciated to be matched by the consumption of the cooling device.

Exergy loss defined in Eq. (45) determines the amount of energy lost due to irreversibilities in the system. **Figure 8a** shows its behavior for the PV+TEC hybrid system as temperature decreases; being obvious that cooling helps reduce the system's exergy losses for three types of PV panels, excepting CdTe. Nonetheless, as shown in **Figure 8a** the total exergy delivered by the system results in a negative amount for CIGS, c-Si, and a-Si. This model is backed by the data found in **Figure 7a**, **b**, and **c**, establishing that, in these cases, the system demands more energy for operation than it generates.

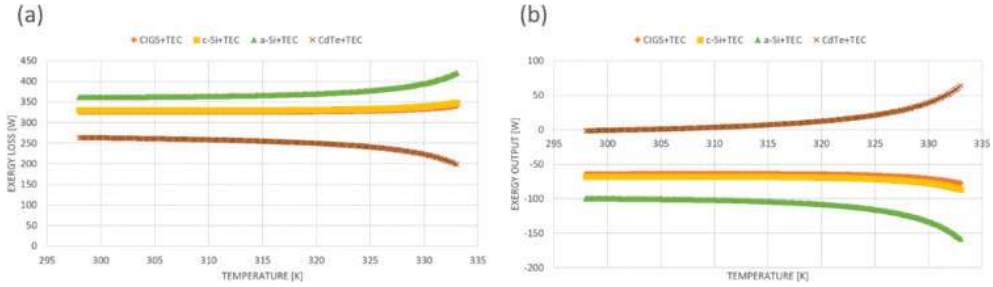

Figure 8. The exergy loss and exergy output for the proposed PV+TEC systems. (a) Exergy loss of OV+TEC systems, (b) Exergy output of OV+TEC systems.

On the other hand, CdTe+TEC system shows to decrease the exergy loss at high ΔT values. The high efficient material properties of the CdTe panel not only locate it in the least exergy loss at all temperature ranges, but also, supported by **Figure 8a** information, indicate that less exergy is used to feed the TEC, as ΔT increases. We must remember that exergy was defined as useful work in Eq. (44), meaning that feeding a cooling system destroys exergy, which is reflected in **Figure 8b**.

These numbers are consistent with the deficit in the exergy output. Only at some ranges, CdTe generates enough energy to result in positive values. TEC consumption increment elevates exergy losses up to a 32.77% at low ΔT values. Furthermore, at high ΔT, exergy loss is decreased, and exergy output is maximized.

For CIGS, c-Si, and a-Si group, cooling increases exergy output generation: 13.69% for CIGS, 21.42% for c-Si, and 36.92% for a-Si as shown in **Figure 8b**. Also, exergy losses can be noted to diminish with the system cooling, 4.03% for CIGS, with a minimum exergy loss temperature range from 313.8 to 305.7 K; 5.34% for c-Si with a minimum exergy loss temperature range from 310.8 to 301.0 K; 13.91% for a-Si with a minimum exergy loss temperature from 298.8 to 298.0 K. It is to be noted that every temperature range where exergy loss is minimal differs from reference or ambient temperatures for PV panels, meaning that excessive cooling can also be counterproductive.

5. Conclusions

In this chapter we have shown that, if we consider the power consumption of the thermoelectric modules, the general energy balance for the whole hybrid PV+TEC system results in a higher energy consumption than energy generation for most systems. Additionally, the exergy analysis shows that for this system there will always be exergy loss, rendering the feasibility of the hybrid PV+TEC system impossible.

Also, the conditions for minimum exergy loss have been determined for diverse types of PV panels, while using thermoelectric cooling modules to decrease temperature. These temperature ranges can be considered as the optimal working conditions, and they all differ from the lowest temperature analyzed for CIGS, a-Si, and c-Si, meaning that reducing the system all the way to ambient temperature (T_{amb}) is not necessarily the best energetic option for the hybrid systems. It is to be noted that this temperature ranges of minimum exergy loss are held within realistic parameters that can be obtained for the system.

We have concluded from these simulation results that the PV+TEC hybrid system is not a viable self-sustaining system. Even though the self-sustenance of the hybrid PV+TEC system is inviable, the conditions for minimum exergy loss allow us to determine the best performance of the system. These optimal operational conditions can be observed from the obtained results, with minimum exergy losses, that can be useful in future studies.

Although the results show that hybrid PV + TEC systems are inviable, thermoelectric technology has a wide range of impact from electronics and telecommunications to medical

equipment. Mostly employed for temperature control of critical parts and components of different lathes and machines; as a cooling method it is precise and reliable technology, with a fluid free compact design requiring only current and voltage for its operation which are easily regulated.

This work shows that a more detailed analysis must be included for the realistic implementation of thermoelectric cooling in photovoltaics. Most works have been realized considering thermoelectric generating (TEG) modules, and just a few around TECs, where an obvious lack of attention has come to the power consumed by the TECs.

Acknowledgements

This work was financially supported by research grant 20180069 of Instituto Politecnico Nacional, México. Arturo Monedero Khouri was financially supported by CONACyT-Mexico (CVU No. 785068). The authors acknowledge the editorial assistance in improving the manuscript.

Author details

Arturo Monedero Khouri and Miguel Angel Olivares Robles*

*Address all correspondence to: olivares@ipn.mx

Instituto Politecnico Nacional, SEPI-ESIME Culhuacan, Coyoacan, Ciudad de Mexico, Mexico

References

[1] Luque A, Hegedus S. Handbook of Photovoltaic Science and Engineering. 1st ed. Chichester: Wiley; 2003

[2] Bellis M. History: Photovoltaics Timeline [Internet]. 2017. Available from: https://www.thoughtco.com/photovoltaics-timeline-1992481 [Accessed: 14-10-2017]

[3] Sears F, Zemansky F, Young H. University Physics. 12th ed. Boston: Addison Wesley; 2009

[4] Khan Academy. Photoelectric Principle [Internet]. 2015. Available from: https://www.khanacademy.org/science/physics/quantum-physics/photons/a/photoelectric-effect [Accesssed: 29-10-2017]

[5] Skopalki E, Palyvos J. On the temperature dependence of photovoltaic module electrical performance: A review of efficiency/power correlations. Solar Energy. 2009;**83**:614-624. DOI: 10.1016/j.solener.2008.10.008

[6] Boxwell M. Solar Electricity Handbook. 11th ed. Birmingham: Greenstream Publishing; 2017

[7] Dorobantu L, Popescu M. Increasing the efficiency of photovoltaic panels through cooling water film. Scientific Bulletin. 2013;**75**:223-232

[8] Irwan Y, Leow M, Irwanto M, Fareq A, Amelia N, Gomesh N, Safwati I. Indoor test performance of PV panel through water cooling method. Energy Procedia. 2015;**79**:604-611. DOI: 10.1016/j.egypro.2015.11.540

[9] Mittleman G, Kribus A, Dayan A. Solar cooling with concentrating photovoltaic/thermal (CPVT) systems. Energy Conversion and Management. 2007;**48**:2481-2490. DOI: 10.1016/j.econman.2007.04.004

[10] Teo H, Li P, Hawlader M. An active cooling for photovoltaic modules. Applied Energy. 2012;**90**:309-315. DOI: 10.1016/j.apenergy.2011.01.017

[11] Rowe D, editor. Handbook of Thermoelectrics. 1st ed. London: CRC Press; 1995

[12] Brazier K. Seebeck Effect [Internet]. 2008. Available from: https://en.wikipedia.org/wiki/File:Thermoelectric_Generator_Diagram.svg [Accesssed: 11-12-2017]

[13] Brazier K. Peltier Effect [Internet]. 2008. Available from: https://en.wikipedia.org/wiki/File:Thermoelectric_Cooler_Diagram.svg [Accesssed: 11-12-2017]

[14] Melcor. Thermoelectric Handbook. 1st ed. Trenton: Laird Technologies; 2015

[15] Cengel Y, Boles M. Thermodynamics, an Engineering Approach. 7th ed. New York: MrGraw Hill; 2011

[16] Van Sark W. Feasibility of photovoltaic-Thermoelectric hybrid modules. Applied Energy. 2011;**88**:2785-2790. DOI: 10.1016/j.apenergy.2011.02.008

[17] Schiro F, Benatto A, Stopatto, Destro N. Improving photovoltaics efficiency by water cooling: Modelling and experimental approach. Energy. DOI: 10.1016/j.energy.2017.04.164

[18] Armstrong S, Hurley W. A model for photovoltaic panels under varying atmospheric conditions. Applied Thermal Engineering. 2010;**30**:1488-1495. DOI: 10.1016/j.applthermaleng.2010.03.012

[19] Sharples S, Charlesworth P. Full-scale measurements of wind-induced convective heat transfer from a roof-roof mounted plate solar collector. Solar Energy. 1998;**83**:187-192. DOI: 10.1016/S0038-092X(97)00119-9

[20] Incropera F, De Witt D. Fundamentals of Heat and Mass Transfer. 7th ed. New Jersey: Wiley; 2011

[21] Kraus A, Bejan A, editors. Heat Transfer Handbook. 1st ed. New Jersey: Wiley; 2003

[22] Cengel Y, Ghajar A. Heat and Mass Transfer. 4th ed. Mexico City: McGraw Hill; 2011

[23] Najafi H, Woodbury K. Optimization of cooling system based on Peltier effect for photovoltaic cells. Solar Energy. 2013;**91**:152-160. DOI: 10.1016/j.solener.2013.01.026

[24] Borkar D, Prayagi S, Gotmare J. Performance evaluation of photovoltaic solar panel using thermoelectric cooling. International Journal of Environmental Research. 2014;**9**:536-539 ISSN: 2319-5013

[25] Kane A, Verma V. Performance enhancement of building integrated photovoltaic module using thermoelectric cooling. International Journal of Renewable Energy Research. 2013;**3**: 320-324 ISSN: 1309-0127

[26] Benghanem A, Al-Mashraqui A, Daffalah K. Performance of solar cells using thermoelectric module in hot sites. Renewable Energy. 2015;**89**:51-59. DOI: 10.1016/j.renene.2015.12.011

[27] Bjørk R, Nielsen K. The performance of a combined photovoltaic (PV) and thermoelectric generator (TEG) system. Solar Energy. 2015;**120**:187-194. DOI: 10.1016/j.solener.2015.07.035

[28] Petela R. Exergy analysis of the solar cylindrical-parabolic cooker. Solar Energy. 2005;**79**: 221-233. DOI: 10.1016/j.solener.2004.12.001

[29] Petela R. Exergy of Heat Radiation. Journal of Heat Transfer. 1964;**86**:187-192. DOI: 10.1115/1.3687092